Geophysical Research Letters

RESEARCH LETTER
10.1029/2018GL081382

Observing the Local Emergence of the Southern Ocean Residual-Mean Circulation

F. Sévellec[1,2], A. C. Naveira Garabato[2], C. Vic[2], and N. Ducousso[1]

[1]Laboratoire d'Océanographie Physique et Spatiale, CNRS Université-Brest IRD Ifremer, Brest, France, [2]Ocean and Earth Science, University of Southampton, Southampton, UK

Key Points:
- Horizontal buoyancy advection by mesoscale eddies at a Southern Ocean mooring site balances mean vertical advection on time scale of 100 days
- The overturning circulation of the Southern Ocean emerges on this time scale as a residual between the eddy-induced and Eulerian-mean flows
- The eddy-induced flow can be accurately parameterized with a Gent-McWilliams diffusivity of ~2,000 $m^2\ s^{-1}$

Supporting Information:
- Supporting Information S1

Correspondence to:
F. Sévellec,
florian.sevellec@univ-brest.fr

Citation:
Sévellec, F., Naveira Garabato, A. C., Vic, C., & Ducousso, N. (2019). Observing the local emergence of the Southern Ocean residual-mean circulation. *Geophysical Research Letters*, *46*, 3862–3870. https://doi.org/10.1029/2018GL081382

Received 19 NOV 2018
Accepted 4 MAR 2019
Accepted article online 7 MAR 2019
Published online 4 APR 2019

Abstract The role of mesoscale turbulence in maintaining the mean buoyancy structure and overturning circulation of the Southern Ocean is investigated through a 2-year-long, single-mooring record of measurements in Drake Passage. The buoyancy budget of the area is successively assessed within the Eulerian and the Temporal-Residual-Mean frameworks. We find that a regime change occurs on time scales of 1 to 100 days, characteristic of mesoscale dynamics, whereby the eddy-induced turbulent horizontal advection balances the vertical buoyancy advection by the mean flow. We use these diagnostics to reconstruct the region's overturning circulation, which is found to entail an equatorward downwelling of Antarctic Intermediate and Bottom Waters and a poleward upwelling of Circumpolar Deep Water. The estimated eddy-induced flow can be accurately parameterized via the Gent-McWilliams closure by adopting a diffusivity of ~2,000 $m^2\ s^{-1}$ with a middepth increase to 2,500 $m^2\ s^{-1}$ at 2,100 m, immediately underneath the maximum interior stratification.

Plain Language Summary In this study we use a 2-year-long, high-resolution (both temporally and vertically) mooring together with a state-of-the-art method (Temporal-Residual-Mean framework) to disentangle the role of mesoscale eddy turbulence for sustaining the Meridional Overturning Circulation leeward of the Drake Passage. Because of its role in carbon sequestration and ocean heat uptake the Meridional Overturning Circulation is a key component of the climate system. However, it is driven by a wide range of physical processes from persistent, large-scale wind to mesoscale and small-scale turbulence. Hence, disentangling how these processes contribute to the maintenance of this climatically relevant ocean circulation is one of the current challenges in physical oceanography. Here we apply a state-of-the-art method (Temporal-Residual-Mean framework) and show the emergence of a balance between mesoscale eddies and Eulerian-mean circulation for buoyancy advection. In particular, we demonstrate that the effect mesoscale eddies can be accurately parameterized with a Gent-McWilliams type diffusivity of ~2,000 $m^2\ s^{-1}$. Beyond this result, this study also provides an observational evidence of the typical large-scale picture of the Meridional Overturning Circulation and shows its relevance at local scales.

1. Introduction

The Southern Ocean plays a pivotal role in the global ocean circulation by connecting the Indian, Pacific, and Atlantic basins (Schmitz, 1996), and the ocean's deep and surface layers (Lumpkin & Speer, 2007). The regional circulation is shaped by physical processes acting on a wide range of spatiotemporal scales—from large-scale, persistent Ekman flows, directly linked to surface wind forcing, to mesoscale and small-scale turbulent motions (Speer et al., 2000). Assessing the relative contributions of, and interplay between, this spectrum of flows in determining the Southern Ocean limb of the Meridional Overturning Circulation (MOC) remains an important open question, with implications for global ocean heat uptake (Liu et al., 2018) and sequestration of carbon dioxide (Landschützer et al., 2015), for instance. However, a complete assessment of these dynamics and their effects is outstanding due to the difficulty of rigorously distinguishing between averaged quantities (produced through inaccurate diagnostic) and mixed quantities (produced through actual mixing). Averaged quantities can be likened to the development of a blurred picture in photography when an overly long exposure time is used to capture a moving object. Hence, unlike mixed quantities, they are the outcome of an inaccurate observation rather than a property of the observed system. The erroneous interpretation of averaged quantities as mixed quantities has been rationalized in the context of the time-mean ocean circulation through the temporal-residual-mean (TRM) framework put forward by McDougall and McIntosh (2001).

Here, we acknowledge this issue, by examining and quantifying the way in which the mean buoyancy structure and overturning circulation are established at a Southern Ocean site, where a mooring was deployed for 2 years. This also allows us to estimate the eddy-induced Gent-McWilliams diffusivities. To conclude, a discussion of the impact of our observational results for our understanding and numerical model representation of the Southern Ocean limb of the MOC is provided.

2. Two Distinct Buoyancy Budget Regimes

To assess the contributions of motions of different scales to sustaining the extension of the MOC across the Southern Ocean, we used in situ observations from a mooring located in the Antarctic Circumpolar Current (ACC) at 56°S, 57°50′W (Figure 1a), leeward of the Drake Passage (see Figure 1a and Brearley et al., 2013 for details of the exact location). These 2-year-long measurements were part of a six-mooring cluster deployed under the auspices of the Diapycnal and Isopycnal Mixing Experiment in the Southern Ocean (DIMES; Naveira Garabato, 2010; Meredith, 2011). This study uses colocated horizonal velocity, temperature, salinity, and pressure data at 1200-, 1299-, 1853-, 1951-, 2049-, 2152-, 3400-, 3600-m depth (see Text S1 in the supporting information for further details). From these observations, vertical velocities can be inferred, and the terms of a time-mean buoyancy budget can be diagnosed. The method to compute vertical velocities from single-mooring measurements is described in Sévellec et al. (2015) and summarized in Text S2; the mean statistical properties of the observational record are shown in Figures 1b–1g. Taking advantage of the equivalent barotropic nature of the ACC flow (Killworth & Hughes, 2002), we defined gradients in the along and across directions of the time- and depth-mean flow (as indicated in Figure 1a). This enables us to eliminate contributions to the buoyancy budget from the time-mean flow in the across direction (Figure 1c), except for a small baroclinic component.

Since the measurements were obtained at broadly constant depth levels, it is natural to compute the buoyancy balance in an Eulerian framework with fixed depths. We start from the buoyancy conservation equation:

$$\partial_t b + u\partial_x b + v\partial_y b + w\partial_z b = 0, \tag{1}$$

where t is time; x, y, and z are the along, across, and vertical directions; b is the buoyancy; and u, v, and w are the along, across, and vertical velocities. By applying a Reynolds decomposition, set for a range of averaging periods (from 15 min to ∼2 years), we separate mean quantities from fluctuations. Taking the overall long-time mean of this decomposition allows us to build a mean buoyancy budget, which intrinsically depends on the averaging/filtering period (as described in Text S3). This can be expressed in terms of mean and turbulent advection as

$$\mathrm{Mean}_{\mathrm{hor}}(\tau,z) + \mathrm{Mean}_{\mathrm{ver}}(\tau,z) \simeq \mathrm{Turb}_{\mathrm{hor}}(\tau,z) + \mathrm{Turb}_{\mathrm{ver}}(\tau,z), \tag{2}$$

where τ is the averaging period, $\mathrm{Mean}_{\mathrm{hor}}$ and $\mathrm{Mean}_{\mathrm{ver}}$ are the mean horizontal and vertical advection of buoyancy, and $\mathrm{Turb}_{\mathrm{hor}}$ and $\mathrm{Turb}_{\mathrm{ver}}$ are the turbulent horizontal and vertical advection of buoyancy, respectively. The mean buoyancy budget measures the relative contribution of the turbulent/fluctuation and mean terms in setting the long-time-mean equilibrium. It also shows how these contributions depend on the averaging/filtering period used in the Reynolds decomposition. Note that there is also a trend term in (1) compared to (2); however, it is negligible at all depths and for all averaging time scales by construction of the mean buoyancy budget (Text S3).

The resulting buoyancy advective terms are enhanced in the upper part of the measured water column, between 1,000 and 2,000 m (Figure 2), where buoyancy gradients, and notably vertical stratification, attain maximum values (Figure 1). The turbulent vertical advection (Figure 2d) is negligible at all depths and for all averaging periods. This indicates that variations in vertical velocity and vertical stratification do not correlate highly enough to sustain a net turbulent advection, despite their substantial magnitudes compared to their mean values (Figures 1d and 1g). In contrast, the mean vertical advection induces a buoyancy gain between 1,000 and 2,000 m (Figure 2b). This is consistent with a mean downwelling of buoyant water: a downward mean vertical velocity through a positive vertical stratification. The mean downwelling is robust to changes in averaging period, confirming the steadiness of this buoyancy flux.

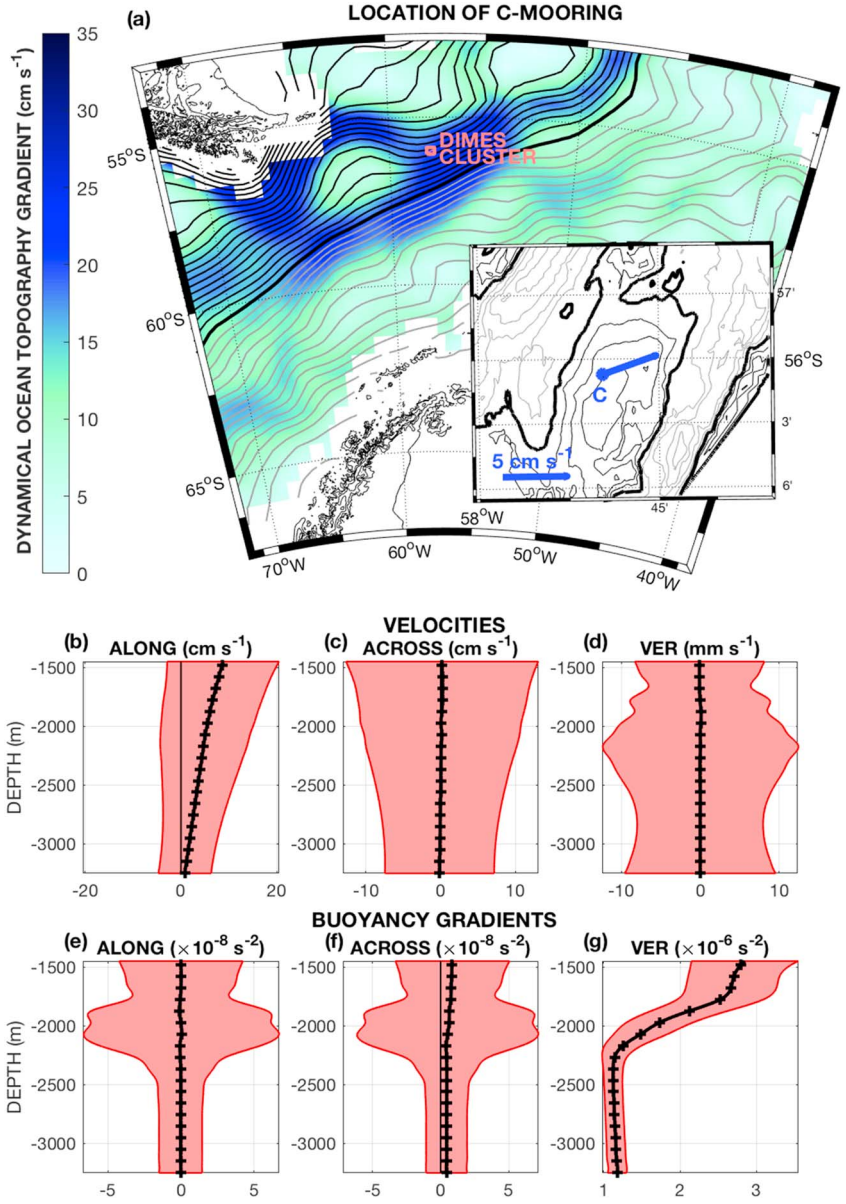

Figure 1. (a) Location of the DIMES C-mooring, with red square denoting the location of the six-mooring cluster. The inset shows a magnification of the region, with blue circle indicating the mooring site. In the main panel, contours represent the dynamic ocean topography averaged from 1992 to 2002 (Maximenko et al., 2009); the solid thick contour marks −1 m, and solid black and gray contours denote higher and lower values at intervals of 5 cm. Color represents the absolute gradient of dynamic ocean topography rescaled as horizontal geostrophic velocity magnitude. In the inset, the solid thick contours indicate the 4,000-m isobath, and the solid black and gray contours denote shallower and deeper isobaths at intervals of 100 m. The thick blue line shows the time- and depth-averaged direction and magnitude of the flow at the mooring location. This average flow direction defines the along direction used in the remainder of our analysis. The across direction is orthogonal to the along direction. (b) Along, (c) across, and (d) vertical velocities, as well as (e) along, (f) across, and (g) vertical buoyancy gradients at the mooring site. Time-mean values are shown on a uniformly spaced 100-m vertical grid (black crosses), connected by a cubic-spline interpolation (black line). The red shading represents ±1 temporal standard deviation. (Time-mean velocities are also displayed as dashed red lines in Figure 3a.) DIMES = Diapycnal and Isopycnal Mixing Experiment in the Southern Ocean.

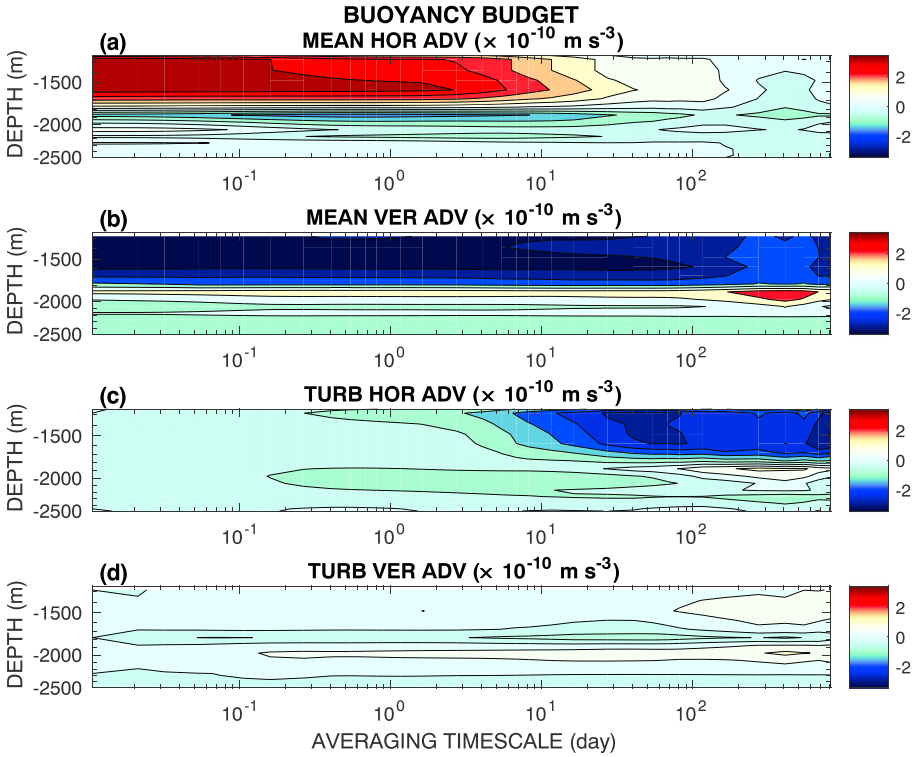

Figure 2. The four components of the buoyancy budget as a function of depth (z) and of the averaging time scale (τ), following (1): (a) mean horizontal advection (Mean_{hor}), (b) mean vertical advection (Mean_{ver}), (c) turbulent horizontal advection (Turb_{hor}), and (d) turbulent vertical advection (Turb_{ver}). Note that $\text{Mean}_{\text{hor}}(\tau,z)+\text{Mean}_{\text{ver}}(\tau,z) \simeq \text{Turb}_{\text{hor}}(\tau,z)+\text{Turb}_{\text{ver}}(\tau,z)$. Both depth and averaging time scale axes follow a log scale. (Here the trend is not shown, since Trend $\simeq 0$.)

The mean horizontal advection induces a buoyancy loss between 1,000 and 2,000 m for averaging periods shorter than 1 day, but is insignificant for periods longer than ~100 days (Figure 2a). This dependency to averaging time scale suggests that this term is not sustained by a steady horizontal flow. Finally, the turbulent horizontal advection also induces a buoyancy loss between 1,000 and 2,000 m (Figure 2c) that emerges for averaging periods longer than ~1 day, converging to a steady value for periods longer than 100 days. This indicates that variations in horizontal velocity (Figures 1b and 1c) and in horizontal buoyancy gradients (Figures 1e and 1f) are significantly correlated on periods between 1 and 100 days.

The preceding Eulerian buoyancy budget exhibits a remarkable dependence on averaging period. Whereas on short time scales the buoyancy balance is between the mean horizontal advection and the mean vertical advection ($\text{Mean}_{\text{hor}}+\text{Mean}_{\text{ver}} \simeq 0$), on long time scales it is the turbulent horizontal advection that balances the mean vertical advection ($\text{Mean}_{\text{ver}} \simeq \text{Turb}_{\text{hor}}$). The change in regime occurs between 1 and 100 days. This time scale is characteristic of mesoscale dynamics, as may be shown, for example, by considering the 6-day propagation time scale derived from the observed zonal propagation speed of mesoscale eddies (2 cm s^{-1}, Klocker & Marshall, 2014) and the baroclinic Rossby deformation radius (10 km, Chelton et al., 1998) characteristic of the ACC. Accordingly, variability within this time scale will be referred to as mesoscale turbulence in the remainder of this study (Klocker & Abernathey, 2014).

The permanent regime is reached for averaging periods of 100 days. This convergence time scale was reported by Sévellec et al. (2015) in a previous investigation of regional dynamics. This period is linked to the cumulative effect of mesoscale eddies propagating over the mooring site and defines the minimum time over which measurements of eddy variables must be acquired to obtain robust statistics and a convergence of the buoyancy budget. This is symptomatic of the central role of eddies in sustaining the turbulent horizontal advection. On time scales of 100 days, a balance is established between mean vertical advection leading to a buoyancy gain and turbulent horizontal advection inducing a buoyancy loss, in the depth range between 1,000 and 2,000 m (Figure 2). This is consistent with the prevalent view of the Southern Ocean limb of the

MOC equatorward of the ACC's axis, where the mooring is located (i.e., equatorward of the maximum gradient of dynamic ocean topography, Figure 1a). In this area, buoyant waters are expected to be downwelled by the mean vertical circulation; this effect is balanced by the mesoscale eddies inducing a sink of buoyancy at depth (Marshall & Radko, 2003, 2006; Toggweiler & Samuels, 1995, 1998). If ergodicity of the ACC flow is assumed (i.e., if time averaging may be considered as equivalent to spatial averaging), our observational diagnostics indicate that mean downwelling at the ACC's northern edge (which represents the equatorward, downwelling branch of the "Deacon cell," Döös & Webb, 1994) is compensated by horizontal mesoscale eddy turbulence.

3. The Residual-Mean Circulation

Having documented the pivotal role of turbulent horizontal advection on time scales longer than 100 days in balancing persistent downwelling, we will test how the former is represented within the TRM framework (McDougall & McIntosh, 1996, 2001). This will enable us to characterize the physical nature of turbulent horizontal advection. In particular, we will assess the extent to which the turbulent buoyancy flux may be accurately parameterized in terms of an adiabatic advection, which has been regularly assumed to prevail over diabatic processes (Gent & McWilliams, 1990). This parameterization often entails the addition of an eddy-induced velocity proportional to the mean isopycnal slope (Gent & McWilliams, 1990). In assessing this parameterization approach, we will mainly concentrate on the permanent regime (i.e., the longest time average).

We apply the TRM framework and compute the quasi-Stokes velocities, as initially suggested by McDougall and McIntosh (1996) and elaborated by McDougall and McIntosh (2001), and summarized in Text S4. We obtain the eddy-induced velocities in the along and across directions of the time- and depth-mean flow (respectively referred to as along- and across-eddy-induced velocities henceforth), and in the vertical direction (Figure 3a). The along-eddy-induced velocities are small compared to the mean along velocities (Figure 3a1), indicating that the residual along transport is mainly determined by the intense mean flow along the path of the ACC. For the across direction, the residual velocities (computed as the sum of the mean and eddy-induced velocities) are determined primarily by the eddy-induced velocities and exhibit a substantial baroclinic structure (Figure 3a2). This suggests that the residual across transport is dominated by the integrated effect of turbulent processes. In turn, vertical eddy-induced velocities are of similar intensity to the vertical mean velocities (Figure 3a3). This results in a significant compensation of the mean and eddy-induced vertical velocities at all depths, which leads to the occurrence of small residual vertical velocities (Figure 3a3). Thus, the vertical transport of buoyancy is significantly weaker than suggested by the mean vertical velocities because of the opposing contribution of eddy-induced flows. This local result is consistent with the common, general circulation model-based view of the residual-mean circulation in the Southern Ocean, in which the Eulerian-mean vertical flow is almost perfectly balanced by the eddy-induced flow (i.e., the vanishing of the Deacon cell in the residual-mean framework, Döös & Webb, 1994; McIntosh & McDougall, 1996). Overall, along residual velocities are of the order of tens of centimeters per second, across residual velocities are of the order of centimeters per second, and vertical residual velocities are of the order of tenths of millimeters per second.

Using these eddy velocities we can express the buoyancy balance within the TRM framework as follows: Trnd + Hor + Ver = 0, where Trnd is the trend of modified buoyancy ($\hat{b} = \bar{b} + \tilde{b}$, the three terms denoting the modified buoyancy, mean buoyancy, and the rescaled buoyancy variance), Hor = $\hat{u}\partial_x\hat{b} + \hat{v}\partial_y\hat{b}$, and Ver = $\hat{w}\partial_z\hat{b}$ (where $\hat{u} = \bar{u} + \tilde{u}, \hat{v} = \bar{v} + \tilde{v}$, and $\hat{w} = \bar{w} + \tilde{w}$ are residual, mean, and eddy-induced along, across, and vertical velocities). Closer examination of this buoyancy balance reveals that the trend of modified buoyancy is small compared to the horizontal and vertical advection of modified buoyancy, which tend to mutually compensate (Figure 3b1). Vertical and horizontal fluxes of buoyancy are decomposed into four terms, in accordance with the TRM framework of McDougall and McIntosh (2001) and as summarized in Text S4. These terms correspond to the following: mean advection of mean buoyancy (MAM); turbulent advection of mean buoyancy (TAM); mean advection of rescaled buoyancy variance (MAV); and turbulent advection of rescaled buoyancy variance (TAV); such that $\mathrm{MAM}_{\mathrm{ver}} = \bar{w}\partial_z\bar{b}$, $\mathrm{TAM}_{\mathrm{ver}} = \tilde{w}\partial_z\bar{b}$, $\mathrm{MAV}_{\mathrm{ver}} = \bar{w}\partial_z\tilde{b}$, and $\mathrm{TAV}_{\mathrm{ver}} = \tilde{w}\partial_z\tilde{b}$ (and equivalently for the horizontal terms).

From this diagnostic, we find that the horizontal buoyancy flux is primarily determined by the mean and turbulent advection of mean buoyancy and by the mean advection of rescaled buoyancy variance, with a

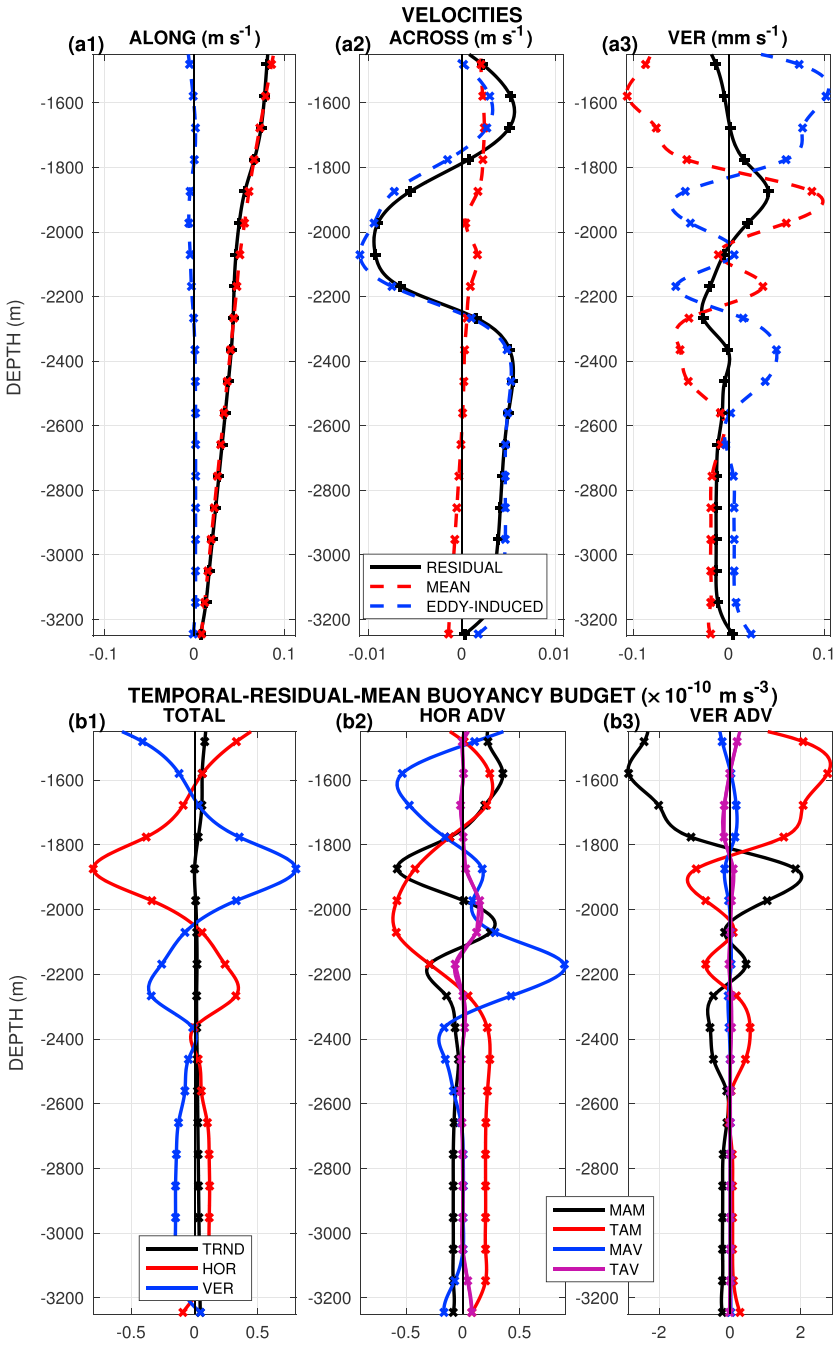

Figure 3. (a1) Along, (a2) across, and (a3) vertical velocities for the (red dashed line) time mean, (blue dashed line) eddy-induced, and (black solid line) residual components for the longest averaging time scale ($\tau = t_2 - t_1 \simeq 2$ years). Eddy-induced velocity is computed through the quasi-Stokes velocity of the Temporal-Residual-Mean framework, and the residual velocity is the sum of the time-mean and eddy-induced velocities. (b1–b3) Buoyancy budget within the Temporal-Residual-Mean framework as a function of depth for the longest averaging time scale ($\tau = t_2 - t_1 \simeq 2$ years). (b1) Total buoyancy budget between the trend (TRND, black line), horizontal advection (HOR, red line), and vertical advection (VER, blue line). (b2 and b3) Horizontal and vertical buoyancy advection balance between the mean advection of mean buoyancy (MAM, black lines), the turbulent advection of mean buoyancy (TAM, red lines), the mean advection of rescaled buoyancy variance (MAV, blue lines), and the turbulent advection of rescaled buoyancy variance (TAV, purple lines). The results are shown on a uniformly spaced 100-m vertical grid (crosses) and are connected by a cubic spline interpolation (line).

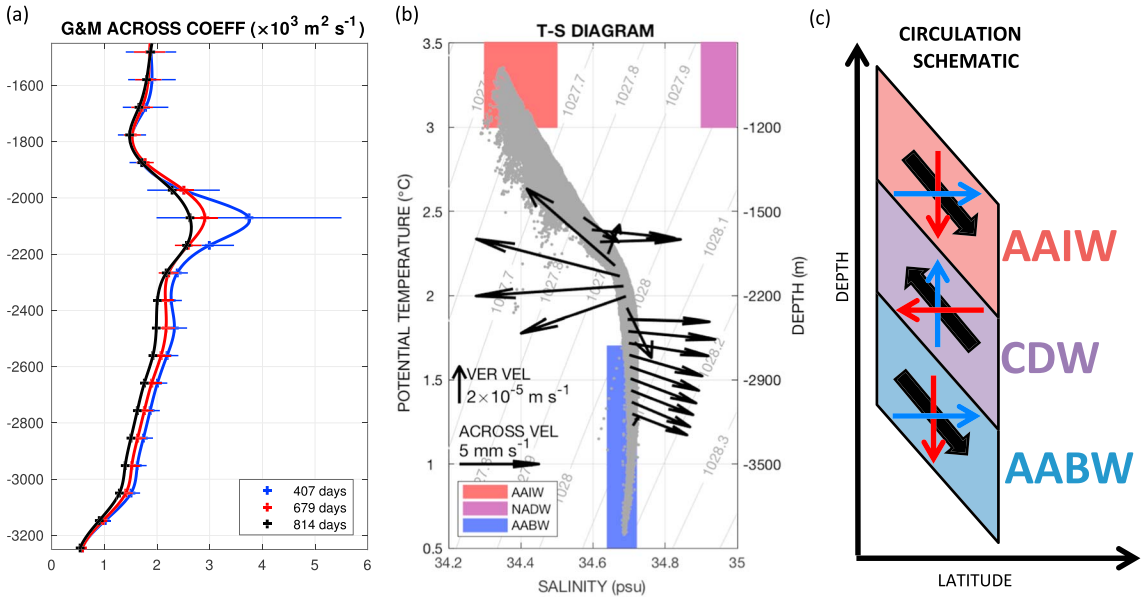

Figure 4. (a) Coefficients for the Gent-McWilliams turbulent closure for eddy-induced velocities for the across direction. Coefficients are computed for averaging timescales of (blue) 407 days, (red) 679 days and (black) 814 days (i.e., the longest averaging timescale). The mean results are shown on a uniformly spaced 100-meter vertical grid (crosses) and are connected by a cubic spline interpolation (line), with uncertainties (horizontal lines correspond to plus/minus one standard deviation). (b) Temperature-Salinity diagram of the mooring measurements (gray dots) including neutral density at a mean depth of 2,360 m (gray contours) and with the corresponding three water types: Antarctic Intermediate Water (AAIW, red patch), North Atlantic Deep Water (NADW, purple patch), and Antarctic Bottom Water (AABW, blue patch). The residual-mean across and vertical velocities (black arrows) are shown at the location of the time-mean temperature and salinity. Depth of the time-mean temperature is indicated for reference. (c) Schematic of the ocean circulation at the mooring location. A three-layer system is maintained through a balance between buoyancy loss and gain (blue and red arrows, respectively) by horizontal and vertical advection (horizontal and vertical colored arrows, respectively). This leads to an overall residual-mean circulation of three water masses (black thick arrows) consisting of equatorward downwelling of AAIW and AABW and a poleward upwelling of CDW (Circumpolar Deep Water).

negligible contribution of the turbulent advection of rescaled buoyancy variance (Figure 3b2). In contrast, the vertical buoyancy flux is dominated by the contribution of the mean and turbulent advection of mean buoyancy, with negligible influence from the mean and turbulent advection of rescaled buoyancy variance (Figure 3b3). Note that the vertical advection terms are one order of magnitude larger than their horizontal advection counterparts (Figure 3b2 versus Figure 3b3). To summarize, the TRM framework indicates that the mean vertical advection of mean buoyancy and the turbulent vertical advection of mean buoyancy dominate the overall buoyancy balance and act to compensate one another.

Now that the eddy-induced velocities and associated buoyancy fluxes have been derived and described, we can compute the eddy-induced velocity coefficients required in the Gent and McWilliams (1990) parameterization. The mathematical description of this procedure is summarized in Text S4.

We find that the eddy-induced velocity coefficients for the across direction (relative to the time- and depth-mean flow, as above) range from 500 to almost 2,500 $m^2\ s^{-1}$ (Figure 4a), and vary widely in the vertical. These values are consistent with the ones used in numerical models including the Gent and McWilliams (1990) closure (e.g., 2,000 $m^2\ s^{-1}$ for NEMO in its 2° × 2° configuration, Madec, 2008; Madec & Imbard, 1996), or those diagnosed in regional eddy-resolving models of the North Atlantic (500 and 2,000 $m^2\ s^{-1}$, Eden et al., 2007) or the California Current System (from 300 to 750 $m^2\ s^{-1}$, Colas et al., 2013), for instance. Following an abrupt increase from 500 $m^2\ s^{-1}$ at 3,200 m to 1,500 $m^2\ s^{-1}$ at 3,000-m depth, the across coefficient increases linearly up to 2,000 $m^2\ s^{-1}$ at 2,300 m. Directly underneath the maximum deep stratification, the coefficient reaches its peak to values up to 2,500 $m^2\ s^{-1}$ at 2,100 m (Figure 1g versus Figure 4a). At shallower levels, the coefficient remains almost constant at 1,800 $m^2\ s^{-1}$ all the way to the upper ocean. Notably, we find that the closure converges when the time-averaging period is increased (Figure 4a).

4. Discussion and Conclusions

Our analysis of a mooring in the ACC reveals that a regime shift in the buoyancy balance occurs between 1 and 100 days, associated with the emergence of mesoscale dynamics. A time scale of 100 days characterizes

the convergence of flow statistics, and corresponds to the minimum time required for enough mesoscale eddy features to propagate past the mooring. On this and longer time scales, an Eulerian buoyancy budget shows that the mean vertical advection of buoyancy is balanced by turbulent horizontal advection. The latter arises from velocities and buoyancy gradients evolving on time scales ranging from 1 to 100 days, characteristic of the mesoscale eddy field. The O(1 day) time scale over which the regime change starts can be used to objectively distinguish between the eddying regime and the noneddying regime in ocean models. Indeed, using an estimate of the speed of first-baroclinic, nondispersive internal gravity waves (NH/π = 0.55 m s^{-1}, where N=1.7 × 10^{-3} s^{-1} and H=1,000 m following Figure 1g) and the longest time scale for which the turbulent horizontal advection (i.e., the use of a turbulent closure) is negligible ($1/f \simeq$0.1 day, Figure 2c), we obtain 0.55 × 8,640 = 5,000 m or ∼1/13° at the mooring latitude, which broadly corresponds to the first-baroclinic Rossby deformation radius. This value is significantly smaller than typical horizontal resolutions adopted by global climate models (∼1/4° at best) but is close to those used in recent global ocean models (∼1/12° at best, except for a few specific studies). This suggests that to accurately represent the buoyancy balance and residual circulation of the Southern Ocean, models require a horizontal resolution of a few kilometers or a robust turbulent closure for the effects of mesoscale eddy flows.

To validate this type of closure against observations, we quantified the eddy-induced circulation through the quasi-Stokes velocities of the TRM framework (McDougall & McIntosh, 2001). We find that the mean horizontal velocities are only weakly modified by the eddy-induced velocities along the direction of the time- and depth-mean flow, whereas eddy-induced velocities dominate for the across direction. This leads to a significant residual-mean horizontal transport across the direction of the time- and depth-mean flow (of the order of centimeters per second). In contrast, the mean vertical velocities are strongly compensated by the eddy-induced velocities. This leads to a weak residual-mean vertical transport. The TRM view of the buoyancy balance differs from the Eulerian view. In the former (which distinguishes averaged quantities from mixed quantities, unlike the Eulerian framework), the buoyancy balance is primarily established between the mean vertical advection of mean buoyancy and the turbulent vertical advection of mean buoyancy.

Finally, we considered a parameterization of the eddy-induced circulation as a purely advective process. Following Gent and McWilliams (1990), the quasi-Stokes velocity is set proportional to the mean isopycnal slope (computed for the modified buoyancy, McDougall & McIntosh, 2001). This leads to across eddy-induced velocity coefficients of ∼2,000 m^2 s^{-1}, but varying by up to a factor 5 over the 2,000-m depth range examined. Our analysis also shows an enhancement of the coefficient up to 2,500 m^2 s^{-1} at a depth of 2,100 m immediately below the maximum of deep stratification.

All in all, our analysis suggests the existence of a residual-mean circulation that redistributes buoyancy vertically and in the across direction. Mapping the residual-mean flow onto the temperature-salinity relation measured by the moored instrumentation, we can diagnose the motion of the three major water masses present at the mooring location: Antarctic Intermediate Water (AAIW), upper and lower Circumpolar Deep Water (CDW), and Antarctic Bottom Water (AABW). These three water masses are derived from three distinct water types (temperature-salinity properties at their origin/formation): AAIW defined in the range of 3–7 °C and 34.3–34.5 psu (Carter et al., 2009), North Atlantic Deep Water defined in the range of 3–4 °C and 34.9–35 psu (Defant, 1961), and AABW defined in the range of −0.9–1.7 °C and 34.64–34.72 psu by (Emery & Meincke, 1986). Following the density classes set by these three water types, we find that AAIW (lightest layer) flows downward and equatorward, CDW (high-salinity layer) flows upward and poleward, and AABW (densest layer) flows downward and equatorward (Figure 4b). In this way, the classical description of the large-scale overturning circulation of the Southern Ocean (Schmitz, 1996; Speer et al., 2000), derived largely from analyses of basin- or global-scale water mass property distributions and general circulation models, is seen to emerge from local measurements of the buoyancy balance (Figure 4c).

Acknowledgments
This research was supported by the Natural Environment Research Council of the U.K. through the DIMES (NE/F020252/1) and SMURPHS (NE/N005767/1) projects. A. C. N. G. acknowledges the support of the Royal Society and the Wolfson Foundation. F. S. acknowledges the DECLIC and Meso-Var-Clim projects funded through the French CNRS/INSU/LEFE program.

References

Brearley, J. A., Sheen, K. L., Naveira Garabato, A. C., Smeed, D. A., & Waterman, S. (2013). Eddy-induced modulation of turbulent dissipation over rough topography in the Southern Ocean. *Journal of Physical Oceanography*, *43*, 2288–2308.

Carter, L., McCave, I. N., & Williams, M. J. M. (2009). Circulation and water masses of the Southern Ocean: A review. *Developments in Earth & Environmental Science*, *8*, 85–114.

Chelton, D. B., deSzoeke, R. A., Schlax, M. G., El Naggar, K., & Siwertz, N. (1998). Geographical variability of the first baroclinic Rossby radius of deformation. *Journal of Physical Oceanography*, *28*, 433–460.

Colas, F., Capet, X., McWilliams, J. C., & Li, Z. (2013). Mesoscale eddy buoyancy flux and eddy-induced circulation in eastern boundary currents. *Journal of Physical Oceanography*, *43*, 1073–1095.
Defant, A. (1961). *Physical oceanography* (p. 182). London: Pergmon Press.
Döös, K., & Webb, D. J. (1994). The deacon cell and the other meridional cells of the Southern Ocean. *Journal of Physical Oceanography*, *24*, 429–442.
Eden, C., Greatbach, R. J., & Willebrand, J. (2007). A diagnosis of thickness fluxes in an eddy-resolving model. *Journal of Physical Oceanography*, *37*, 727–742.
Emery, W. J., & Meincke, J. (1986). Global water masses: Summary and review. *Oceanologica Acta*, *9*, 383–391.
Garabato Naveira, A. C. (2010). Cruise report RRS James Cook jc041 (DIMES UK1) 5 Dec 2009 to 21 Dec 2009 (Tech. Rep.). National Oceanography Centre Southampton Cruise Rep. 164pp.
Gent, P. R., & McWilliams, J. C. (1990). Isopycnal mixing in ocean circulation model. *Journal of Physical Oceanography*, *20*, 150–155.
Killworth, P. D., & Hughes, C. W. (2002). The antarctic circumpolar current as a free equivalent-barotropic jet. *Journal of Marine Research*, *60*, 19–45.
Klocker, A., & Abernathey, R. (2014). Global patterns of mesoscale eddy properties and diffusivities. *Journal of Physical Oceanography*, *44*, 1030–1046.
Klocker, A., & Marshall, D. P. (2014). Advection of baroclinic eddies by depth mean flow. *Geophysical Research Letters*, *41*, 3517–3521. https://doi.org/10.1002/2014GL060001
Landschützer, P., Gruber, N., Haumann, F. A., Rödenbeck, C., Bakker, S., Heuven, D. C. E., et al. (2015). The reinvigoration of the Southern Ocean carbon sink. *Nature*, *349*, 1221–1224.
Liu, W., Lu, J., Xie, J.-P., & Fedorov, A. V. (2018). Southern Ocean heat uptake, redistribution and storage in a warming climate: The role of meridional overturning circulation. *Journal of Climate*, *31*, 4727–4743. https://doi.org/10.1175/JCLI-D-17-0761.1
Lumpkin, R., & Speer, K. (2007). Global ocean meridional overturning. *Journal of Physical Oceanography*, *37*, 2550–2562.
Madec, G. (2008). Nemo ocean engine (Tech. Rep.). France: Institut Pierre-Simon Laplace (IPSL). No27, 332pp.
Madec, G., & Imbard, M. (1996). A global ocean mesh to overcome the North Pole singularity. *Climate Dynamics*, *12*, 381–388.
Marshall, J., & Radko, T. (2003). Residual-mean solutions for the Antarctic circumpolar current and its associated overturning circulation. *Journal of Physical Oceanography*, *33*, 2341–2354.
Marshall, J., & Radko, T. (2006). A model of the upper branch of the meridional overturning of the Southern Ocean. *Progress in Oceanography*, *70*, 331–345.
Maximenko, N., Niiler, P., Rio, M.-H., Melnichenko, O., Centurioni, L., Chambers, D., et al. (2009). Mean dynamic topography of the ocean derived from satellite and drifting buoy data using three different techniques. *Journal of Atmospheric and Oceanic Technology*, *26*, 1910–1919.
McDougall, T. J., & McIntosh, P. C. (1996). The temporal-residual-mean velocity. Part I: Derivation and scalar conservation equations. *Journal of Physical Oceanography*, *26*, 2653–2665.
McDougall, T. J., & McIntosh, P. C. (2001). The temporal-residual-mean velocity. Part II: Isopycnal interpretation and the tracer and momentum equations. *Journal of Physical Oceanography*, *31*, 1222–1246.
McIntosh, P. C., & McDougall, T. J. (1996). Isopycnal averaging and the residual mean circulation. *Journal of Physical Oceanography*, *26*, 1655–1660.
Meredith, M. P. (2011). Cruise report: RRS James Cook JC054 (DIMES UK2) 30 Nov 2010 to 8 Jan 2011. (Tech. Rep.). British Antarctic Survey Cruise Rep. 206pp.
Schmitz, W. J. (1996). On the world ocean circulation: Volume II (Tech. Rep.). Woods Hole Oceanographic Institution. 237pp.
Sévellec, F., Naveira Garrabato, A. C., Brearley, J. A., & Sheen, K. L. (2015). Vertical flow in the Southern Ocean estimated from individual moorings. *Journal of Physical Oceanography*, *45*, 2209–2220.
Speer, K., Rintoul, S. R., & Sloyan, B. (2000). The diabatic deacon cell. *Journal of Physical Oceanography*, *30*, 3212–322.
Toggweiler, J. R., & Samuels, B. (1995). Effect of Drake Passage on the global thermohaline circulation. *Deep-Sea Research Part I*, *42*, 477–500.
Toggweiler, J. R., & Samuels, B. (1998). On the ocean's large-scale circulation near the limit of no vertical mixing. *Journal of Physical Oceanography*, *28*, 1832–1852.

Reference From the Supporting Information

McDougall, T. J., & Barker, P. M. (2011). Getting started with TEOS-10 and the Gibbs Seawater (GSW) oceanographic toolbox (Tech. Rep.) SCOR/IAPSOWG127.